Pergamon

0967–0645(95)00043–7

Deep-Sea Research II, Vol. 42, No. 2–3, pp. 777–804, 1995
Copyright © 1995 Elsevier Science Ltd
Printed in Great Britain. All rights reserved
0967–0645/95 $9.50 + 0.00

Regional estimates of the export flux of particulate organic carbon derived from thorium-234 during the JGOFS EqPac program

KEN O. BUESSELER,* JOHN A. ANDREWS,* MARY C. HARTMAN,* REBECCA BELASTOCK* and FEI CHAI†

(*Received* 27 *April* 1994; *in revised form* 15 *October* 1994; *accepted* 2 *February* 1995)

Abstract—The upper ocean ^{234}Th activity distribution at 77 stations was measured between 12°N and 10°S, and 95°W and 170°W in the spring and autumn of 1992. A regional scavenging model was used to estimate vertical export of particulate ^{234}Th. Given the relatively high upwelling rates in this region, particularly at equatorial latitudes near 140°W, it was necessary to include upwelling of ^{234}Th in our model in order to quantify particulate export. Using this export flux and the measured organic C or N to ^{234}Th ratio on particles, one can empirically determine POC and PON fluxes for this region. The estimated particulate organic C flux varies spatially and temporally within this region, ranging from 1 to 7 mmol C m^{-2} day^{-1}, with enhanced export occurring over the equator. Fluxes are also enhanced along 95°W coincident with a low temperature/high nutrient peak at 4°S. Along 140°W, particulate organic C export from the upper 100 m is on the order of 2 mmol C m^{-2} day^{-1} at latitudes beyond 4°N and 4°S, with an equatorial peak of 3–5 mmol C m^{-2} day^{-1} in both spring and fall. These results suggest that a relatively small per cent of the total production is exported locally on sinking particles (particle export/primary production <5–10%). This finding of low particle export is relatively insensitive to the chosen upwelling rates or particulate organic C/^{234}Th ratios. Given the measured C/N ratio, particulate N fluxes from the upper 100 m would be 6 times lower than for POC.

INTRODUCTION

Satellite composites of ocean color show an extensive band of high surface pigment concentration in the equatorial Pacific. These images suggest that the Pacific is an important region of enhanced phytoplankton production and carbon fixation. Previous studies of primary production and "new" production (i.e. that fraction of production supported by nutrient inputs from outside the euphotic zone) indicate that 18–56% of global new production occurs in the equatorial Pacific (Chavez and Barber, 1987). Recent modeling efforts suggest that much of the new production may be removed as dissolved organic matter (DOM) and not as particulate organic carbon (POC) as previously assumed (Toggweiler, 1989; Legendre and Gosselin, 1989; Bacastow and Maier-Reimer, 1991). The surface waters of the equatorial Pacific are characterized by high pCO_2 levels, which

*Department of Marine Chemistry and Geochemistry, Woods Hole Oceanographic Institution, Woods Hole, MA 02543, U.S.A.
†University of Maine, Orono, ME 04469, U.S.A.

lead to the outgassing of 0.8–1.0 × 10^9 tons of carbon per year during non-El Niño periods (Feely *et al.*, 1995). Quantifying the equatorial Pacific's role in the global carbon budget and further understanding the extent to which CO_2 fixed during primary production is removed as a POC or DOM flux are two primary goals of the NOAA and NSF-sponsored JGOFS (Joint Global Ocean Flux Study) EqPac (Equatorial Pacific) program (Murray *et al.*, 1922, 1994).

We report here on our results using thorium-234 (^{234}Th) to quantify the particulate flux of organic C and N from the upper 100 m in the equatorial Pacific in 1992. Thorium-234 is a naturally occurring particle-reactive radionuclide ($t_{\frac{1}{2}}$ = 24.1 days) that has been widely used to study particle scavenging processes in the upper ocean (Bhat *et al.*, 1969; Santschi *et al.*, 1979; Minagawa and Tsunogai, 1980; Kaufman *et al.*, 1981; Coale and Bruland, 1985, 1987; Murray *et al.*, 1989). The use of ^{234}Th to determine organic C and N particle fluxes is based upon recent work conducted during the JGOFS North Atlantic Bloom Experiment (NABE, Buesseler *et al.*, 1992a). In the NABE, profiles of ^{234}Th and a non-steady-state scavenging model were used to quantify particulate ^{234}Th fluxes. Using the ratio of POC or PON to particulate ^{234}Th, Buesseler *et al.* (1992a) were able to empirically determine the export fluxes of POC and PON. Confidence in this approach was obtained by the close agreement found between the ^{234}Th derived fluxes and independent estimates of export during the NABE (CO_2 and nutrient balances).

Our goal for the EqPac program was to obtain an estimate of particulate organic carbon fluxes on a much larger spatial scale than had been attempted during the NABE. To meet this goal, we collected samples at a total of 77 stations located between 12°N and 10°S latitude and 95°W and 170°W longitude during 6 cruises in early and late 1992. To reduce wire time and the overall sample load, we developed a vertically integrated sampling approach, whereby the average concentrations of dissolved and particulate ^{234}Th for the 0–100 m layer were determined at each station from *in situ* pump samples. Also, rather than relying on sediment trap data or separate bottle casts for the ratio of POC and PON to particulate ^{234}Th, we measured this ratio directly on the same filters for two size classes of particles (>53 μm and >0.7–53 μm). Both a traditional vertical scavenging model and a 3-D regional ^{234}Th flux model were used. In the regional model, seasonally adjusted 1992 horizontal and vertical transport velocities plus the measured horizontal and vertical ^{234}Th gradients are used to calculate export fluxes. Using the particulate organic C, N and ^{234}Th data, sinking fluxes of C and N can then be calculated. The sensitivity of these models was tested by making initial comparisons to estimates of total production and export reported by other EqPac investigators.

SAMPLING AND ANALYSES

Sampling locations

Samples were collected on 6 legs of the NOAA sponsored JGOFS EqPac cruises in 1992. Legs 1–3 were conducted aboard the R.V. *Malcolm Baldridge* during the northern hemisphere spring, while legs 4–6 were conducted aboard the R.V. *Discoverer* in the fall/winter months. In general, transects were made between 10°S and 12°N on four meridional lines in the region of 95–170°W. NOAA stations were typically separated by 1 degree latitude beyond 2°N and 2°S, with stations as close as 0.25 degrees latitude near the equator. We sampled for ^{234}Th at a subset of these stations, with up to 12 stations per meridional transect. The spring cruises included transects along 110°W and 125°W (Leg 1, 1–21 March, dates for ^{234}Th sampling), 170°W (Leg 2, 4–14 April), and 140°W (Leg 3, 26 April–5 May). The fall cruises went only as far west as 140°W (Leg 4, 10–17 September) with additional sampling for ^{234}Th at 125°W (Leg 4, 20 September–2 October), 110°W (Leg 5, 17 October–11 November), and 95°W (Leg 6, 29 November–2 December).

Vertically integrated sampling

To increase our spatial coverage for ^{234}Th, a novel vertically integrated sampling strategy was employed to reduce the total number of samples, relative to traditional profiling. An *in situ* pump was lowered and raised on an independent winch at a constant speed between fixed depths, while maintaining a constant flow rate for the pump. Typically, we sampled from the surface to 100 m (measured by an *in situ* pressure sensor) by lowering and raising the pump through two cycles between the surface and depth over a 2 h period. With this strategy it was felt that highly stratified features in the ^{234}Th or particulate C or N profiles would not be missed, and that the data would best represent average concentrations in the 0–100 m layer. This sampling strategy is in some ways analogous to the horizontal integrating techniques used by Ledwell *et al.* (1991) for following purposeful tracer releases in the oceans. We used a similar vertically integrating approach during a time-series 3-D sampling study, where multiple ^{234}Th determinations were required to calibrate upper ocean sediment traps off Bermuda (Buesseler *et al.*, 1994).

On the first of the six legs, the maximum depth of sampling was based upon the depth of the euphotic zone (always < 100 m). This was determined by the depth of the 1% light level, or at night, by estimation from previous stations. On all other legs, vertically integrated samples were taken from either the surface to 100 m, or as paired samples from 1–50 m and 50–100 m at some of the 2°N and 2°S stations. Fixed depth samples also were collected at about 1/3 of the stations to assess the variation in particulate organic C and N to ^{234}Th ratios with depth and to establish total ^{234}Th activities at the base of the 0–100 m layer (see below). All original data have been submitted to the NOAA data base (J. Hendee, Data Manager, NOAA/AOML) and are summarized here in Tables 1 and 2 as averages for the 0–100 m layer.

In situ *pumping*

Sample volumes of 300–600 liters were processed at flow rates of 3–5 liters min^{-1}. The inlet of the pump consisted of a 142 mm diameter PVC filter holder with a 130 mm wide opening machined out of a single 5 cm tall cover plate and penetrated by numerous 1 cm diameter holes. This design is operationally similar to the baffled filter holder used on the pumping system designed by Bishop and Edmond (1976). In this manner, the sample was evenly distributed across the filter surface and the particles more gently drawn onto the entire surface of the 142 mm diameter filters. Due to the baffles, the filtered particles were protected from washing off the prefilter during pump retrieval. The filter holder was designed so that two filters could be placed in series, separated by a 3 cm spacer and plastic support grid. We used a 53 μm pore Nitex screen as the prefilter, followed by an 0.7 μm pore GFF filter for all particulate samples. We use the terms LPOC and LPON (large particulate organic C or N) to refer to organic C and N data from those particles retained

Table 1. Thorium-234 data for 0–100 m layer

Lat (deg N)	Long (deg W)	Collection date	Time (GMT)	STA No.	CAST No.	NOAA LOG No.	Mean salinity (ppt)	Dissolved ^{234}Th (dpm l^{-1})	± error	GFF ^{234}Th (dpm l^{-1})	± error	Nitex ^{234}Th (dpm l^{-1})	± error
12	110	01/03/92	23:41	2	8	920612317	34.19	1.50	0.16	0.64	0.05	0.036	0.001
10	110	02/03/92	13:23	3	11	920621230	34.13	1.45	0.10	0.59	0.04	0.025	0.002
8	110	03/03/92	04:38	4	18	920630352	34.38	1.37	0.16	0.47	0.03	0.048	0.003
5	110	04/03/92	05:14	6	25	920640414	34.57	1.42	0.15	0.51	0.04	0.079	0.004
2	110	05/03/92	18.59	9	38	920651804	34.70	1.33	0.22	0.82	0.06	0.032	0.003
1	110	06/03/92	04:38	10	41	920660340	34.77	1.31	0.19	0.80	0.05	0.051	0.001
0	110	06/03/92	17:36	13	48	920661635	35.12	1.34	0.12	0.55	0.04	0.062	0.004
−1	110	07/03/92	11:07	16	55	920671012	35.14	1.21	0.20	0.83	0.06	0.070	0.003
−2	110	07/03/92	22:38	17	61	920672137	35.13	1.32	0.26	0.77	0.05	0.047	0.002
−5	110	08/03/92	01:00	20	70	920682347	35.54	1.08	0.16	0.97	0.06	0.064	0.003
−8	110	11/03/92	05:25	22	83	920710424	35.55	1.23	0.15	0.82	0.05	0.067	0.003
10	125	21/03/92	01:13	42	156	920810014	34.40	1.51	0.12	0.46	0.04	0.047	0.004
8	125	02/03/92	12:16	41	149	920801120	34.54	1.12	0.13	0.83	0.20	0.020	0.002
5	125	19/03/92	12:17	39	139	920791100	34.69	1.32	0.09	0.47	0.13	0.043	0.002
2	125	18/03/92	11:36	36	130	920781038	34.80	1.23	0.21	0.47	0.10	0.227	0.007
1	125	18/03/92	03:05	35	127	920780205	34.95	1.49	0.11	0.76	0.16	0.073	0.003
0	125	17/03/92	12:30	32	119	920771113	35.13	1.44	0.09	0.48	0.05	0.089	0.001
−1	125	16/03/92	13:00	29	111	920761157	35.05	1.50	0.18	0.39	0.21	0.077	0.005
−2	125	16/03/92	03.52	28	108	920760250	35.09	1.36	0.17	0.68	0.06	0.054	0.000
−5	125	15/03/92	01:52	25	96	920750042	35.40	1.18	0.12	0.86	0.06	0.056	0.001
−8	125	14/03/92	04:34	23	89	920740334	35.81	1.07	0.11	0.98	0.07	0.083	0.003
10	170	04/04/92	20:26	46	175	920951923	34.61	1.17	0.10	0.62	0.05	0.013	0.001
8	170	05/04/92	11:24	47	179	920961011	34.36	1.20	0.17	0.53	0.04	0.033	0.001
5	170	06/04/92	11:09	49	185	920970958	34.63	1.34	0.11	0.65	0.06	0.029	0.002
2	170	07/04/92	13:13	52	195	920981227	34.95	1.21	0.09	0.76	0.05	0.069	0.002
1	170	07/04/92	23:22	53	200	920982144	34.89	1.08	0.09	0.76	0.06	0.053	0.001
0	170	08/04/92	21:06	56	206	920991954	34.79	1.14	0.11	0.52	0.05	0.078	0.002
−1	170	10/04/92	03:25	59	218	921010236	34.77	0.95	0.12	0.74	0.06	0.029	0.002
−2	170	10/04/92	15:37	60	223	921011456	35.06	0.85	0.10	0.81	0.05	0.076	0.003
−5	170	11/04/92	14:24	63	231	921021324	35.15	0.87	0.10	0.77	0.06	0.071	0.001
−8	170	12/04/92	17:33	65	241	921031616	35.30	1.00	0.09	0.81	0.06	0.056	0.002
−10	170	13/04/92	08:58	66	246	921040800	35.54	0.77	0.09	1.00	0.08	0.075	0.004
10	140	05/05/92	20:30	89	334	921261945	34.47	1.28	0.12	0.63	0.05	0.032	0.001
9	140	05/05/92	11:25	88	329	921261030	34.67	1.14	0.12	0.70	0.05	0.041	0.001
5	140	03/05/92	11:10	85	316	921241020	34.71	1.09	0.13	0.59	0.05	0.077	0.001
2	140	02/05/92	11:05	82	307	921231010	34.78	1.22	0.11	0.56	0.04	0.032	0.003
1	140	01/05/92	10:30	81	301	921221000	35.03	1.08	0.12	0.50	0.05	0.054	0.004
0	140	30/04/92	09:25	78	293	921210750	35.17	1.43	0.10	0.43	0.04	0.088	0.001

−1	140	29/04/92	06:23	75	284	921200515	35.21	1.24	0.11	0.61	0.04	0.077	0.003
−2	140	28/04/92	20:53	74	278	921191950	35.11	1.22	0.09	0.59	0.04	0.037	0.015
−5	140	27/04/92	07:45	71	266	921180644	35.38	0.94	0.09	0.88	0.07	0.068	0.001
−7	140	26/04/92	04:25	69	257	921170327	35.70	0.69	0.09	1.28	0.07	0.071	0.002
0	110	13/05/92	08:45	94	346	921340755	34.80	1.21	0.11	0.55	0.04	0.073	0.003
10	140	10/09/92	05:47	2	11	922540638	34.28	1.32	0.09	0.69	0.04	0.024	0.002
9	140	10/09/92	14:47	3	13	922541553	34.32	1.24	0.08	0.74	0.04	0.030	0.002
−5	140	17/09/92	04:30	20	64	922610604	35.35	1.14	0.08	0.62	0.04	0.043	0.003
−7	140	17/09/92	19:10	22	71	922612007	35.37	0.96	0.07	0.62	0.04	0.061	0.001
10	125	02/10/92	03:06	46	171	922760416	34.47	1.24	0.09	0.64	0.04	0.025	0.003
9	125	01/10/92	18:43	45	167	922751942	34.23	1.74	0.21	0.23	0.01	0.006	0.001
8	125	01/10/92	07:35	44	161	922750947	34.26	1.76	0.21	0.19	0.01	0.004	0.001
5	125	29/09/92	11:32	41	148	922731310	34.52	0.98	0.12	0.15	0.01	0.074	0.002
2	125	28/09/92	11:13	38	135	922721201	34.72	1.19	0.11	0.55	0.04	0.105	0.003
1	125	27/09/92	13:34	37	128	922711446	34.76	1.48	0.18	0.15	0.01	0.007	0.001
0	125	26/09/92	09:01	34	120	922700954	35.03	1.87	0.13	0.32	0.02	0.060	0.002
−1	125	25/09/92	11:51	31	117	922691305	35.17	1.35	0.12	0.57	0.04	0.080	0.003
−2	125	24/09/92	03:22	30	109	922681202	35.22	1.20	0.11	0.31	0.02	0.059	0.001
−5	125	23/09/92	09:36	27	95	922671026	35.48	0.99	0.10	0.73	0.04	0.056	0.003
−8	125	21/09/92	12:33	25	83	922651324	35.72	1.29	0.16	0.33	0.02	0.006	0.001
−10	125	20/09/92	23:23	24	82	922650016	35.90	1.47	0.18	0.34	0.02	0.015	0.001
10	110	17/10/92	02:48	50	180	922910128	34.09	1.66	0.11	0.27	0.02	0.028	0.003
8	110	31/10/92	15:36	51	190	923051442	34.03	1.43	0.10	0.34	0.02	0.069	0.001
5	110	01/11/92	11:07	53	197	923061008	34.00	1.05	0.08	0.36	0.02	0.027	0.001
2	110	03/11/92	06:48	56	216	923080552	34.39	1.49	0.09	0.25	0.02	0.059	0.006
1	110	03/11/92	15.39	57	219	923081445	34.61	1.32	0.11	0.39	0.03	0.145	0.017
0	110	04/11/92	05:15	60	225	923090411	34.91	1.66	0.12	0.40	0.03	0.141	0.017
−1	110	06/11/92	08:24	63	238	923110711	35.02	1.85	0.12	0.43	0.03	0.094	0.011
−2	110	07/11/92	01:47	65	245	923120055	34.93	1.35	0.11	0.45	0.04	0.116	0.014
−5	110	08/11/92	15:07	68	259	923131415	35.16	1.53	0.12	0.40	0.03	0.086	0.010
−8	110	09/11/92	13:58	70	271	923141305	35.35	1.10	0.11	0.50	0.04	0.104	0.013
−10	110	10/11/92	05:45	71	279	923150452	35.15	1.16	0.10	0.51	0.04	0.139	0.017
3	95	02/12/92	12:24	107	424	923371131	33.97	1.57	0.12	0.50	0.04	0.050	0.006
2	95	02/12/92	04:13	106	420	923370313	34.01	1.42	0.08	0.40	0.03	0.087	0.008
1	95	01/12/92	18:07	105	415	923361714	34.49	1.27	0.10	0.41	0.03	0.048	0.007
0	95	14/11/92	11:42	73	289	923191116	34.73	1.76	0.12	0.26	0.03	0.035	0.004
−1	95	01/12/92	01:16	103	404	923360024	34.90	1.54	0.11	0.33	0.03	0.046	0.006
−2	95	30/11/92	20:50	102	400	923350958	34.99	1.57	0.12	0.52	0.04	0.062	0.008
−3	95	30/11/92	08:29	101	394	923350736	34.92	1.62	0.12	0.35	0.03	0.064	0.008
−5	95	29/11/92	14:26	99	384	923341428	34.84	1.26	0.10	0.29	0.02	0.034	0.004

All ^{234}Th data decay corrected to time of collection and reported as disintegrations per minute per liter.
Errors for ^{234}Th (± error) are propagated from counting statistics, calibration uncertainty and for dissolved ^{234}Th, Mn cartridge collection efficiency.

Table 2. POC and PON data for 0–100 m *layer*

Lat (deg N)	Long (deg W)	GFF POC (μmol l^{-1})	± error	GFF PON (μmol l^{-1})	± error	Nitex POC (μmol l^{-1})	± error	Nitex PON (μmol l^{-1})	± error
12	110	2.24	0.08	0.355	0.031	0.048	0.029	0.0077	0.0047
10	110	1.71	0.09	0.273	0.023	0.076	0.016	0.0105	0.0012
8	110	2.13	0.11	0.356	0.030	0.141	0.023	0.0233	0.0021
5	110	1.67	0.04	0.227	0.020	0.146	0.021	0.0324	0.0027
2	110	2.22	0.12	0.375	0.032	0.061	0.020	0.0116	0.0014
1	110	1.90	0.11	0.292	0.026	0.051	0.018	0.0081	0.0030
0	110	1.29	0.04	0.205	0.018	0.081	0.018	0.0200	0.0019
−1	110	1.56	0.09	0.256	0.023	0.060	0.020	0.0095	0.0032
−2	110	1.85	0.10	0.269	0.024	0.082	0.019	0.0121	0.0014
−5	110	2.15	0.11	0.321	0.027	0.071	0.016	0.0127	0.0013
−8	110	2.11	0.05	0.286	0.024	0.068	0.016	0.0114	0.0012
10	125	1.93	0.12	0.337	0.032	0.103	0.030	0.0164	0.0049
8	125	1.78	0.10	0.318	0.027	0.056	0.015	0.0109	0.0012
5	125	1.93	0.10	0.351	0.029	0.042	0.013	0.0066	0.0022
2	125	1.99	0.05	0.304	0.026	0.345	0.041	0.0706	0.0056
1	125	2.02	0.11	0.337	0.028	0.094	0.018	0.0191	0.0018
0	125	1.50	0.08	0.293	0.024	0.157	0.020	0.0286	0.0024
−1	125	2.05	0.05	0.301	0.025	0.117	0.019	0.0188	0.0018
−2	125	1.73	0.09	0.280	0.024	0.068	0.015	0.0112	0.0012
−5	125	1.83	0.10	0.266	0.023	0.032	0.014	0.0051	0.0023
−8	125	2.09	0.05	0.267	0.023	0.072	0.018	0.0134	0.0014
10	170	1.35	0.04	0.214	0.023	0.016	0.013	0.0025	0.0021
8	170	1.24	0.07	0.172	0.016	0.017	0.013	0.0027	0.0021
5	170	1.42	0.08	0.221	0.020	0.041	0.015	0.0052	0.0009
2	170	1.61	0.06	0.247	0.018	0.070	0.018	0.0104	0.0025
1	170	1.84	0.10	0.281	0.023	0.034	0.013	0.0088	0.0010
0	170	1.50	0.08	0.266	0.023	0.066	0.017	0.0107	0.0012
−1	170	2.06	0.06	0.327	0.028	0.024	0.020	0.0039	0.0032
−2	170	1.61	0.07	0.285	0.019	0.073	0.017	0.0124	0.0023
−5	170	1.24	0.07	0.251	0.023	0.029	0.017	0.0045	0.0027
−8	170	1.29	0.07	0.263	0.022	0.021	0.013	0.0093	0.0011
−10	170	1.70	0.06	0.270	0.023	0.061	0.021	0.0097	0.0034
10	140	1.19	0.05	0.189	0.017	0.036	0.019	0.0057	0.0031
9	140	1.26	0.05	0.200	0.018	0.017	0.017	0.0027	0.0027
5	140	1.68	0.05	0.267	0.023	0.093	0.022	0.0129	0.0015
2	140	1.43	0.05	0.226	0.019	0.028	0.017	0.0045	0.0027
1	140	1.67	0.07	0.266	0.024	0.069	0.025	0.0110	0.0041
0	140	1.54	0.04	0.255	0.022	0.157	0.022	0.0273	0.0023
−1	140	1.79	0.05	0.277	0.024	0.121	0.020	0.0154	0.0016
−2	140	1.33	0.04	0.212	0.013	0.024	0.009	0.0039	0.0014
−5	140	1.46	0.05	0.231	0.020	0.033	0.017	0.0053	0.0027
−7	140	1.65	0.05	0.261	0.022	0.052	0.018	0.0082	0.0029
0	110	1.49	0.09	0.279	0.024	0.108	0.020	0.0155	0.0016
10	140	1.44	0.02	0.229	0.019	0.002	0.013	0.004	0.0021
9	140	1.10	0.04	0.172	0.016	0.010	0.012	0.0015	0.0020
−5	140	1.62	0.04	0.248	0.021	0.028	0.014	0.0045	0.0022
−7	140	1.69	0.05	0.269	0.024	0.056	0.016	0.0089	0.0027
10	125	1.72	0.05	0.261	0.024	0.025	0.018	0.0040	0.0029
9	125	0.26	0.02	0.041	0.005	bd		bd	

Table 2. Continued

Lat (deg N)	Long (deg W)	GFF POC ($\mu mol\ l^{-1}$)	± error	GFF PON ($\mu mol\ l^{-1}$)	± error	Nitex POC ($\mu mol\ l^{-1}$)	± error	Nitex PON ($\mu mol\ l^{-1}$)	± error
8	125	0.23	0.02	0.036	0.004	bd		bd	
5	125	0.21	0.02	0.033	0.004	bd		bd	
2	125	1.70	0.04	0.273	0.022	0.170	0.019	0.0277	0.0032
1	125	0.24	0.02	0.037	0.004	bd		bd	
0	125	0.87	0.03	0.146	0.013	0.118	0.010	0.0189	0.0016
−1	125	1.69	0.05	0.290	0.025	0.163	0.016	0.0256	0.0023
−2	125	0.77	0.02	0.123	0.009	0.058	0.010	0.0090	0.0015
−5	125	2.06	0.06	0.321	0.028	0.066	0.020	0.0105	0.0032
−8	125	0.54	0.02	0.083	0.009	bd		bd	
−10	125	0.44	0.02	0.070	0.007	bd		bd	
10	110	1.28	0.04	0.203	0.017	0.094	0.014	0.0150	0.0025
8	110	1.04	0.03	0.168	0.015	0.061	0.012	0.0097	0.0020
5	110	1.16	0.03	0.192	0.017	na		na	
2	110	0.76	0.02	0.121	0.008	0.062	0.008	0.0094	0.0011
1	110	1.51	0.04	0.254	0.013	0.254	0.014	0.0404	0.0033
0	110	1.72	0.04	0.276	0.023	0.181	0.014	0.0262	0.0023
−1	110	1.23	0.04	0.211	0.018	0.148	0.012	0.0238	0.0020
−2	110	2.40	0.05	0.381	0.018	0.170	0.016	0.0256	0.0023
−5	110	1.17	0.04	0.203	0.018	0.119	0.012	0.0175	0.0016
−8	110	1.45	0.04	0.248	0.022	0.145	0.015	0.0224	0.0020
−10	110	2.05	0.05	0.355	0.029	0.230	0.015	0.0352	0.0030
3	95	1.66	0.05	0.317	0.027	0.054	0.015	0.0085	0.0025
2	95	1.72	0.04	0.307	0.020	0.136	0.011	0.0191	0.0013
1	95	2.48	0.06	0.477	0.039	0.105	0.016	0.0169	0.0017
0	95	0.86	0.05	0.165	0.019	0.030	0.020	0.0048	0.0032
−1	95	1.69	0.04	0.287	0.024	0.064	0.013	0.0098	0.0011
−2	95	2.26	0.05	0.424	0.034	0.104	0.015	0.0166	0.0016
−3	95	1.69	0.04	0.322	0.027	0.105	0.014	0.0165	0.0016
−5	95	2.13	0.05	0.404	0.033	0.111	0.015	0.0184	0.0017

POC and PON data provided on a carbonate free basis.
Errors on POC and PON propagated from blank corrections and calibrations.
bd = Below detection. na = Not analyzed.

by the Nitex screen; and the standard POC or PON terms to refer to the particles retained on the GFF filter.

Downstream from the filter holder the water passed through a gear pump powered by a conducting cable from the surface. Water exiting the pump passed through two MnO_2 impregnated cartridges, which were used to collect dissolved ^{234}Th from seawater. As shown previously (Livingston and Cochran, 1987; Buesseler *et al.*, 1992b), the activity of dissolved ^{234}Th can be quantified by determining the collection efficiency for dissolved ^{234}Th from the equation

$$\text{Collection efficiency} = 1 - \text{MnB/MnA}$$

where MnA and MnB are the ^{234}Th activities of the first and second Mn cartridge in series, respectively. The overall size of our Mn cartridges was reduced relative to previously published procedures (Buesseler *et al.*, 1992b) by impregnating a 11.5 cm (3.25 inch) tall [vs 25.4 cm (10 inch)], 5 μm pore HYTREX II filter cartridge with MnO_2 (Hartman and Buesseler, 1994). The collection efficiencies follow a normal Gaussian distribution, with a mean collection efficiency of 0.79 ± 9% (n = 103).

Sample handling

The filter holder was drained at the end of each pump cast. All subsequent handling steps were carried out in a covered area on the work bench to minimize the possibility for particulate contamination. Since Nitex is an unsuitable matrix for CHN analyses, a procedure was developed to remove the bulk of the particulate matter from the screen. The Nitex filter was carefully removed, using gloved hands and tweezers, from the filter holder and placed into a 100 ml beaker, rinsed with 50 ml of GFF pre-filtered deep water, and sonified for 30 s. The sample and beaker washes were immediately filtered onto a pre-combusted 25 mm GFF filter under vacuum. The sample and beaker rinses totalled approximately 125 ml for this entire process, and DOC analyses of the initial rinse water and filtrate were conducted to check for loss of organic C during this process. The rinse water was collected within one week of the pump cast and refrigerated between use. All glassware was rinsed with 1 N HCl, Milli-Q water and filtered deep water between samples. In some cases, multiple 25 mm filters were needed to collect all the material rinsed off of a single 142 mm diameter Nitex screen. The loaded 25 mm filters were placed in plastic Petri dishes, dried overnight in a 40–50°C oven, and stored in a desiccator for shore-based analyses.

The 142 mm GFF filters were placed in a holder and two 25 mm diameter sub-samples were cut from each filter using a sharpened stainless steel pipe. These sub-samples, each representing 3.6% of the total filter area, were dried overnight and returned to shore for CHN analyses. The remainder of the GFF filter was folded into a reproducible triangular geometry, placed into a plastic Petri dish, and dried prior to on board gamma counting for ^{234}Th.

The MnO_2 cartridges were dried for 24–48 h in the oven prior to counting on board for ^{234}Th. In order to improve the efficiency of detection of the low energy ^{234}Th gamma-ray emissions, we used a hydraulic press and dye to compress the dried Mn cartridge under 10 tons of pressure for 60 s. This resulted in a reproducible 3 cm tall geometry, which resembled a hockey "puck".

Analyses

Thorium 234. The dried and folded GFF filters and Mn "pucks" were counted directly on a pure Ge gamma detector. We used a CANBERRA 2000 mm^2 LEGe style gamma detector with a J-style 15 liter LN_2 Dewar with a low background option in the ^{234}Th region (background count rate = 0.024 cpm ± 50% at 63.3 keV). The detector was interfaced to a Tennelec power supply, amplifier, and an ORTEC multi channel analyzer board installed in the docking station of a lap-top PC. The entire unit was powered through a UPS power supply. No detectable shifts in peak energies or background count rates were seen during the 180+ days of operation at sea. LN_2 consumption rates of 5–10 liters per week were met with three 35 liter storage Dewars that had a LN_2 loss rate of <0.3 liters day^{-1}. A plastic sample holder positioned the samples over the center of the detector window. A single layer of 3.8 × 7.6 × 15.2 cm (1.5 × 3 × 6 inch) lead bricks with a Cu/Cd liner was used for shielding.

GFF, MnA, and MnB samples were counted for 2 h, 6 h and 12 h, with net count rates of 1–10 cpm, 0.5–4 cpm and <2 cpm, respectively. Each ^{234}Th peak was quantified using our own peak fitting software. Counting errors of less than 10%, 5% and 15% were common for the GFF, MnA, and MnB samples, respectively. The calibration of the detector and initial efficiency was determined by a ^{238}U solution (in equilibrium with ^{234}Th) which was added to blank Mn cartridges and filters. Our final gamma detector efficiencies were determined from analyses of Mn cartridges and filters returned to the lab for radiochemical purification and low level beta counting. Relative to gamma counting, beta counting techniques are much more labor intensive, but have higher counting efficiencies (>50% for beta vs <20% for gamma detectors). The branching ratio for ^{234}Th gamma is also low (3.9% at 63 keV). The overall gamma detection efficiency was 0.063 ± 8.5% (n = 22) for the Mn cartridges, and 0.21 ± 10% (n = 10) for the GFF filters (efficiency = net gamma cpm/(branching ratio × dpm)). In some cases, the Mn cartridges were >3 half-lives old prior to beta counting, and a small correction for supported ^{234}Th due to ingrowth from ^{238}U had to be made. This correction (<5% of signal at t = 80 days) was either due to ^{238}U from seawater remaining in the wet cartridge after deployment or due to a small collection efficiency for dissolved ^{238}U on these Mn cartridges (on the order of 0.5%). Based upon independent analyses of deep ocean samples where ^{234}Th and ^{238}U are known to be in equilibrium, we have calibrated our beta counters to better than ±2% (Buesseler *et al.*, 1994).

The calibration of our gamma system can be checked independently by the analyses of our deepest EqPac samples, where ^{234}Th and ^{238}U should be approaching secular equilibrium. We sampled for total ^{234}Th as deep as 167 m on a single cast and found a ^{234}Th/^{238}U activity ratio of 1.03 ± 0.06. In addition, the ^{234}Th/^{238}U ratio of all of the samples ⩾100 m was found to be 1.03 ± 0.08 (n = 23). This is in good agreement with the EqPac data of Bacon *et al.* (1995).

The Nitex screens had insufficient ^{234}Th activity to allow us to quantify ^{234}Th using direct gamma counting procedures. These samples were returned to the lab for low level beta counting after digestion and radiochemical purification (Buesseler *et al.*, 1992b). In addition, some of the filters were counted directly on beta detectors at WHOI (^{234}Th is the highest abundance beta-emitter in these samples) in an attempt to develop procedures for non-destructive ^{234}Th beta analyses. In every case, we followed the decay of ^{234}Th over 2 half-lives on a single beta detector. A curve fitting procedure was then used to determine the t_0 activity of ^{234}Th with its characteristic 24.1 day half-life. This improves precision and reduces uncertainty on the accuracy of the analyses due to slight variations in detector or sample background.

All of the ^{234}Th data are reported on a disintegration/minute basis (dpm) decay corrected to the mid-point of sample collection. The error on each ^{234}Th activity determination is propagated from the uncertainty of the curve fit to the activity data, the uncertainty on the detector calibration, and for dissolved ^{234}Th, the error associated with determining the collection efficiency using Mn cartridges.

Particulate organic carbon and nitrogen. One of the goals of this study was to directly measure the ratio of organic C and N to ^{234}Th in the suspended and sinking particulate pools. Organic C and N were determined on sub-samples from each filter type using a

Perkin–Elmer 2400 CHN analyzer. For the >0.7–53 μm particles, CHN analyses were conducted on sub-samples of the 142 mm GFF filter. In the case of the >53 μm particles rinsed from the Nitex screen onto a 25 mm GFF filter, a sub-sample of this GFF filter (10–20% by weight) was analyzed. Prior to CHN analyses, we used an acid-fuming step to remove carbonate-C. Thus all data reported here are in units of μmol l^{-1} for the organic C fraction only. A comparison between CHN analyses conducted with and without this acid fuming step indicated that carbonate-C accounts for <8% of total C for the GFF filters ($n = 27$); but for the Nitex screens, the carbonate fraction may be as large as 20% of the total ($n = 13$). Other EqPac data suggest that at specific depths an even greater per cent of the particulate carbon pool in the >53 μm size classes may be carbonate (Bacon *et al.*, 1995).

When the Nitex data were first examined, a systematic trend towards higher C/N ratios for the smallest samples was found. Analyses of field blanks (i.e. field deployments of filters with zero volume pumped) indicated a highly variable and C-rich blank that could be as large as some of the Nitex samples (150 ± 80 μg C and 18 ± 5 μg N per sample). All of the Nitex CHN data were corrected for this field blank and the error was propagated throughout the LPOC and LPON calculations, thus increasing the uncertainty significantly on the smaller samples. Once this field blank was considered, all Nitex particulate samples scattered around a mean C/N molar ratio of 6.4 ± 0.6. We suspect that the blank was either from soot particles or oils that formed as a slick around the ship and were picked up by our filters during the deployment. The field blank correction for our GFF filters was much smaller, and a mean C/N molar ratio of 6.1 ± 0.6 was found on these samples, with a field blank correction of <5% ($n = 77$). The lower limits of detection for C and N are the same; therefore we were limited by the lower abundance of N in marine particles. If the particulate C/N ratio error was >35%, we recalculated PON for that sample using the measured organic C value and a molar C/N ratio of 6.3.

To gain confidence in our LPOC data, we attempted to quantify artifacts related to our rinsing procedure. In the case of both ^{234}Th and POC/PON, the per cent of the total concentration found on the Nitex screen was very small, so incomplete collection of large particles is not a serious issue for mass balance purposes. Since our primary goal is the determination of particulate ^{234}Th to organic C ratios, both ^{234}Th and POC were measured on the exact same fractions. To determine the magnitude of the loss of large particles to the rinse solution, we regularly took separate aliquots of the rinse water and filtrate to ascertain a measurable increase in DOC in the rinse solution. Using high temperature DOC techniques (in collaboration with E. Peltzer), we found a small but highly variable organic C loss to the rinse solution (25 ± 23%, $n = 63$) during both the spring and fall cruises. With regard to the opposite artifact, i.e. the retention of particulate material on the screen, we analyzed 51 rinsed screens for ^{234}Th and found a small but variable ^{234}Th signal from particles retained on the screens after sonification and rinsing (median = 30%). As stated above, neither of these effects should have an impact on measured C/^{234}Th ratio or mass balance results in any significant way. Until we find an appropriate filter for direct analyses of ^{234}Th and CHN on the large size classes, we are forced to rely on some type of procedure for removing the particles off of the Nitex screen prior to analyses. Ultimately, our *in situ* filtration and processing procedures are an improvement over previous studies where organic C to ^{234}Th ratios were determined from separate casts and different operational collection techniques (comparing traps vs bottle POC vs *in situ* pumping).

RESULTS

The data in this paper are the average concentrations of ^{234}Th and organic C and N for the 0–100 m layer (Tables 1 and 2). We will use the term "spring" to refer to those samples collected between 21 March and 5 May, and "fall" for those collected between 10 September and 2 December. In an attempt to examine regional trends in the data, all data were contoured by a software package (SURFER™ by Golden Software), which uses a Kriging technique to grid the data. The same grid scale (12 × 25) and weighting factors (y:x = 1:3) were used to draw all fields. The contour intervals were chosen to provide easy visual comparison between seasons for any given parameter, and station locations are shown in every case. In presenting the data in this manner, temporal trends are ignored within the 2–3 month time period required to sample all transects, and small-scale concentration gradients associated with individual eddies or other mesoscale features are averaged. In surface temperature data, one clearly sees the transition in 1992 between the generally warmer El Niño-like conditions during the spring cruises, and the cooler waters in the fall indicative of enhanced upwelling at the end of the 1992 El Niño period (Fig. 1). Surface nutrients show a similar pattern, with elevated nutrients associated with cooler temperatures (Murray *et al.*, 1994).

Thorium-234

The total ^{234}Th activities for the 0–100 m layer range between 1.7 and 2.2 dpm l^{-1} in the spring of 1992 with a trend towards higher values in the east (Fig. 2). Along the 110°W, 125°W and 140°W lines higher activities also occur at the northern and southern extremes, but the zonal gradients are not large. Within errors (generally around 8–10% for total ^{234}Th), these activities are significantly lower than the parent ^{238}U activity estimated from salinity (Chen *et al.*, 1986). Salinity variations between the spring and fall are minimal (Table 1), hence the activity of ^{238}U is similar at all sites. On average, by a depth of 100 m equilibrium between ^{238}U and ^{234}Th has been reached.

In the fall, the NOAA sampling program was conducted farther to the east. In addition, equipment problems led to very few stations for ^{234}Th along the 140°W line (n = 4). Total ^{234}Th activities in the 0–100 m layer show a larger range than during the spring, from <1.5 to >2.1 dpm l^{-1} (Fig. 2). Higher activities can be found along, or just south of, the equator, especially in the east. A low ^{234}Th activity region is seen centered around 5°N along the 125 and 110°W transects.

In the spring, a region of high particulate ^{234}Th (>0.7–53 μm) generally occurs along southern latitudes (>0.8 dpm l^{-1}) particularly along the 140°W meridian (Fig. 3). The GFF ^{234}Th represents up to 60% of the total activity (8°N, 140°W), and at its lowest, 20% (1°S, 125°W). In the fall, overall particulate ^{234}Th activities for the GFF filters are lower, ranging from <0.2 to >0.6 dpm l^{-1} (10–40% of the total—Table 1).

Thorium-234 activities for the >53 μm particles represent a small percent of the total (<1–4%) and range in activity from <0.02 to >0.12 dpm l^{-1} (Table 1). In the spring, there is a clear maximum in the large particle ^{234}Th activity at 2°N along the 125°W transect, while in the fall two maxima occur along 110°W centered around the equator and 8°S (Fig. 4). The patterns of both small and large particle size classes differ significantly in both seasons (compare Figs 3 and 4).

All of our ^{234}Th data generally agree with other EqPac results along 140°W reported by

Bacon *et al.* (1995) and Murray *et al.* (1995); however, a direct intercalibration was never conducted. Bacon *et al.* (1995) collected multiple discrete ^{234}Th profiles using *in situ* pumping (surface–4000 m) at the equator at 140°W. Murray *et al.* (1995) collected ^{234}Th from bottle casts (surface–400 m) along the 140°W line. We find no significant difference among these research groups between the average ^{234}Th activities (Δ^{234}Th ≤ 0.1 dpm l^{-1}) for the 0–100 m layer in the spring.

Particulate organic carbon and nitrogen

Organic carbon and nitrogen were measured on two particle size classes: >0.7–53 μm (POC and PON) and >53 μm (LPOC and LPON). Because the ratio of C/N on each size class is constant within our errors (6.3 ± 0.5), we contoured only the POC and LPOC data in which we have higher confidence (Figs 5 and 6). POC concentrations for the 0–100 m layer in the spring range between 1 and 3 μmol l^{-1} (Fig. 5). In the fall, the range is not appreciably higher, but some values <1 μmol l^{-1} are found, particularly along the 125°W line (Fig. 5). The LPOC concentrations are generally <1–3% of total POC. LPOC concentrations range widely, from <0.01 to >0.2 μmol l^{-1} (Fig. 6). The regional pattern of LPOC and the large particle ^{234}Th are similar (compare Figs 4 and 6). Our POC and LPOC concentrations agree in general with EqPac data collected along 140°W from other *in situ* pumping programs (Bacon *et al.*, 1995; Bishop *et al.*, 1995).

DISCUSSION

Flux calculations

The activity balance of total ^{234}Th can be described by the following equation:

$$\partial A_{\mathrm{Th}}/\partial t = A_{\mathrm{U}}\lambda - A_{\mathrm{Th}}\lambda - P + V \tag{1}$$

where $\partial A_{\mathrm{Th}}/\partial t$ is the change in ^{234}Th activity with time, A_{U} is the ^{238}U activity determined from salinity (^{238}U (dpm l^{-1}) = 0.07097 salinity; Chen *et al.*, 1986), A_{Th} is the measured activity of total ^{234}Th, λ is the decay constant for ^{234}Th (= 0.0288 day^{-1}), P is the net removal flux of ^{234}Th on particles, and V is the sum of advective and diffusive terms. Other than *in situ* ^{238}U decay, there are no other significant sources of ^{234}Th in the oceans, such as atmospheric deposition.

We first examine a steady state model that ignores the advective and diffusive terms. It will be shown that ^{234}Th cannot be assumed to be in steady state; however, the physical supply and loss terms cannot be ignored. We therefore have developed a regional 3-D flux model that includes seasonal and site specific upwelling and horizontal fluxes in the overall regional ^{234}Th activity balance. In this case, the particle flux P can be solved from the following equation

$$P = (A_{\mathrm{U}} - A_{\mathrm{Th}})\lambda + w\partial A_{\mathrm{Th}}/\partial z - u\partial A_{\mathrm{Th}}/\partial x - v\partial A_{\mathrm{Th}}/\partial y \tag{2}$$

where w is the upwelling velocity and $\partial A_{\mathrm{Th}}/\partial z$ the vertical gradient in ^{234}Th activity, u is the zonal velocity and $\partial A_{\mathrm{Th}}/\partial x$ the activity gradient from west to east, and v is the meridional velocity and $\partial A_{\mathrm{Th}}/\partial y$ the activity gradient from south to north.

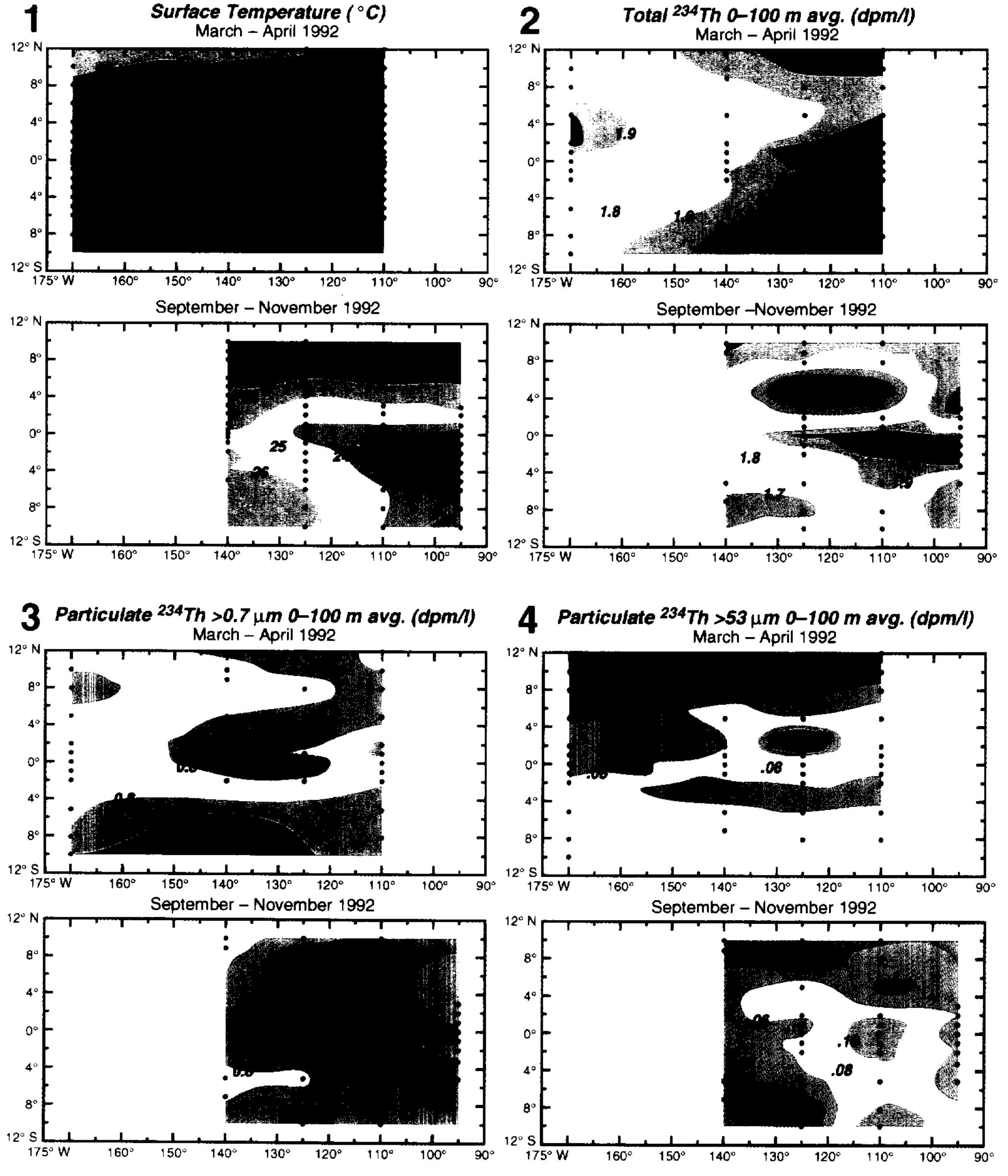

Figs 1–4. Contoured data from spring (upper panel) and fall (lower panel). Station locations are shown as a solid black circle. Fig. 1. Surface temperature map. Fig. 2. Total ^{234}Th for 0–100 m. Fig. 3. Particulate ^{234}Th (>0.7–53 μm) for 0–100 m. Fig. 4. Particulate ^{234}Th (>53 μm) for 0–100 m.

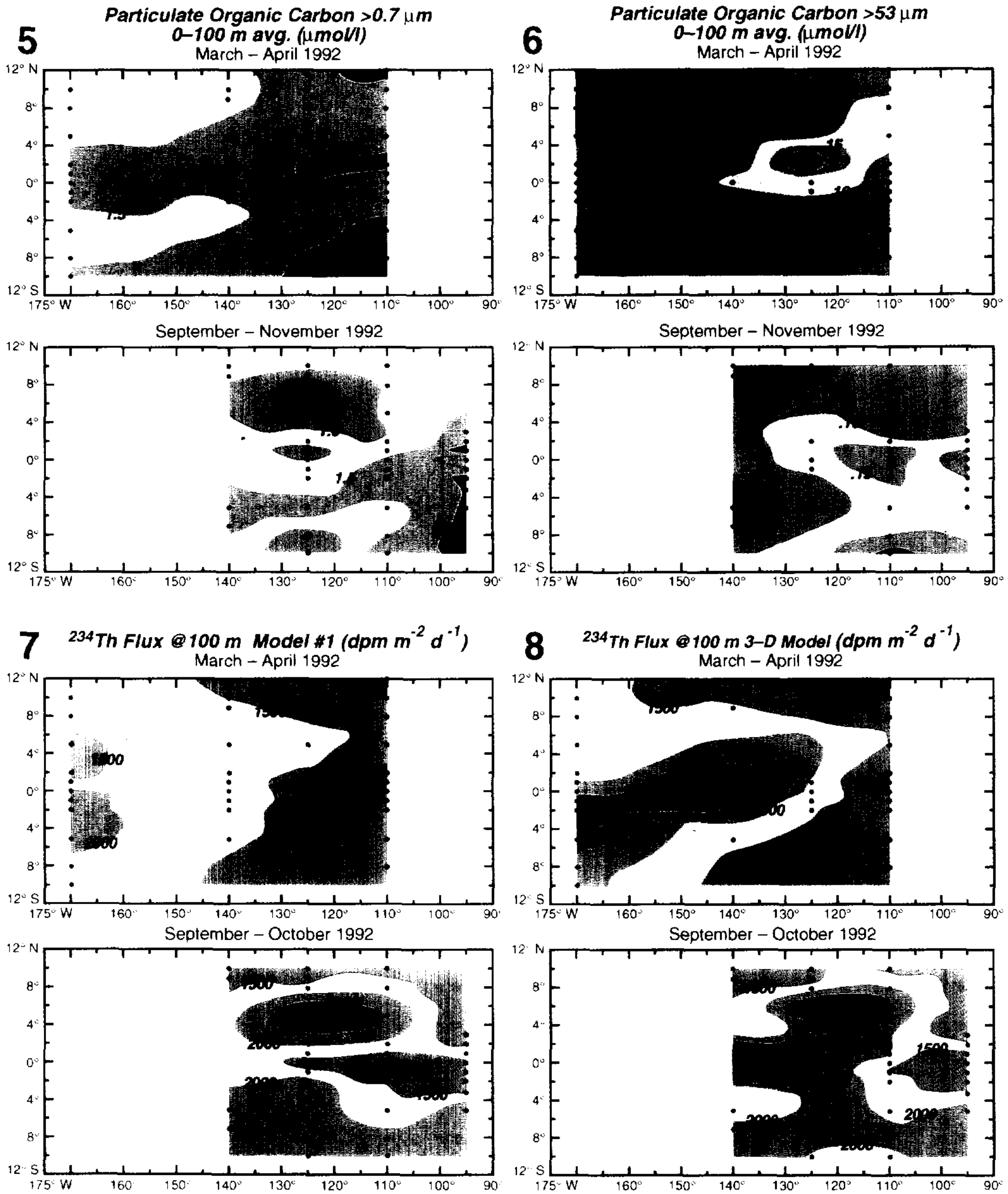

Figs 5–8. Fig. 5. Particulate organic C (>0.7–53 μm) for 0–100 m. Fig. 6. Particulate organic C (>53 μm) for 0–100 m. Fig. 7. Particulate ^{234}Th flux calculated for 100 m from Model No. 1 (advection ignored). Fig. 8. Particulate ^{234}Th flux calculated for 100 m from 3-D regional model.

11

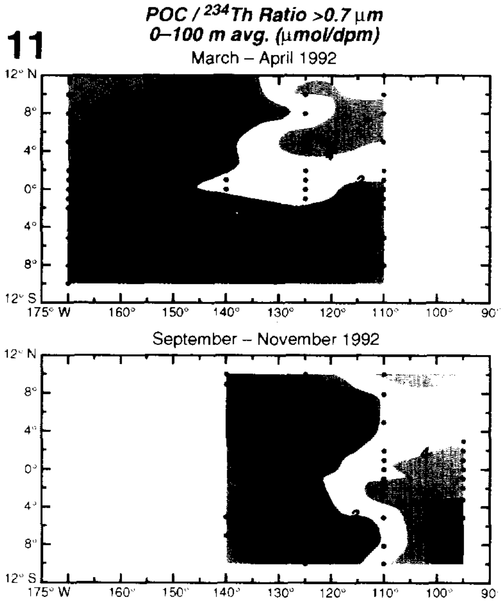

12

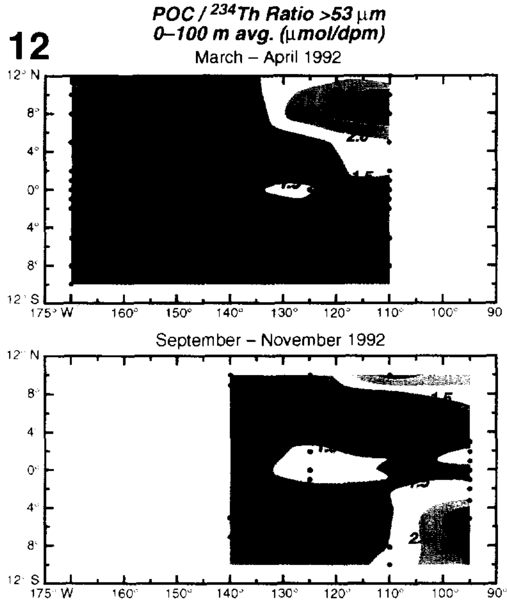

13

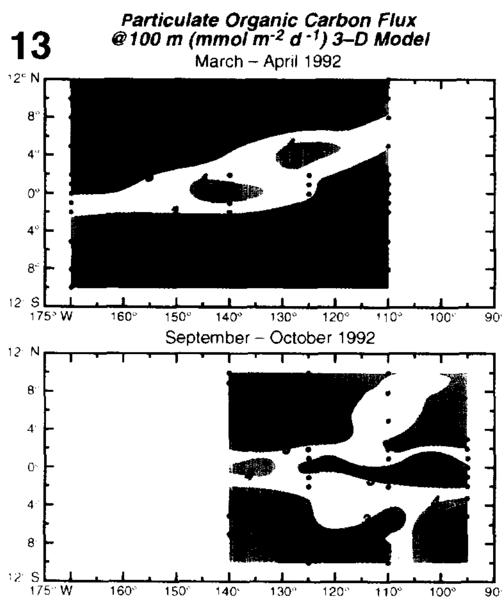

Figs 11–13. Fig. 11. Particulate organic C/^{234}Th ratios for GFF filters for 0–100 m. Fig. 12. Particulate organic C/^{234}Th ratio for Nitex screens (>53 μm) for 0–100 m. Fig. 13. Particulate organic C flux calculated for 100 m using 3-D regional model and LPOC/^{234}Th ratios. Fluxes of PON can be estimated to be a factor of 6.3 lower, given the measured particulate C/N ratio.

^{234}Th export: Model No. 1

Using the data for total ^{234}Th from the upper 100 m, the flux of particulate ^{234}Th can be easily solved using equation (1) assuming steady state and ignoring V. In the study region, salinity increases slightly towards the south along latitudinal bands, corresponding to a ^{238}U activity range between 2.33 and 2.46 dpm l^{-1}. Given that the ^{238}U/salinity relationship has been shown to be accurate to within 1% (Chen *et al.*, 1986), the uncertainty in our flux estimate is dominated by the overall accuracy and precision of the ^{234}Th analyses.

Using this model the ^{234}Th flux pattern is essentially the inverse of the total ^{234}Th activity data (compare Figs 2 and 7). In the spring, this approach predicts a trend towards higher ^{234}Th fluxes in the west, with relatively small latitudinal trends along any given transect. In the fall, the ^{234}Th flux trends are more complex, with a maximum at 5°N between 110 and 125°W and a minimum centered around the equator between 95 and 125°W (Fig. 7).

As pointed out by Coale and Bruland (1987), because the ^{234}Th particle flux is driven by a relatively small difference between two large numbers (i.e. ^{238}U–^{234}Th), the error on the flux estimate increases as the ^{234}Th/^{238}U ratio approaches unity. The overall uncertainty on total ^{234}Th is propagated from counting errors and the uncertainty due to detector calibration and the collection efficiency for dissolved ^{234}Th via our Mn cartridge technique (see Sampling and Analyses). Given uncertainties on total ^{234}Th of 5–8%, our error on P ranges from around $\pm 10\%$ at an activity of 1.5 dpm l^{-1} to $>50\%$ at activities >2.2 dpm l^{-1} (^{234}Th/^{238}U ratio of >0.90). On average, by 100 m we find a ^{234}Th/^{238}U ratio of 1.03 ± 0.08 ($n = 23$). Ratios >1 can be found if surface water ^{234}Th fluxes are large and particles are remineralized at a specific depth at a high rate (i.e. P is negative). During EqPac, we find ^{234}Th/^{238}U ratios as high as 1.2 at 100 m, and our deepest total ^{234}Th sample at 167 m has a ratio indicating secular equilibrium (1.03 ± 0.06). Above the depth of equilibrium, both adsorption onto particle surfaces and losses due to particle disaggregation and desorption occur, but using the single thorium isotope, ^{234}Th, only the net rate of ^{234}Th particle export can be determined.

As stated above, in this simple calculation we ignore both non-steady state effects and advective and diffusive transport. These assumptions are made in most studies, as only single profiles of ^{234}Th are measured and therefore activity gradients in time or space cannot be assessed. Determining the magnitude of $\partial^{234}\mathrm{Th}/\partial t$ proved significant during the NABE, however, where we observed a decrease in ^{234}Th by 0.5 dpm l^{-1} over three weeks that paralleled the depletion of surface nitrate beginning with the onset of the spring bloom (Buesseler *et al.*, 1992a). Even in the NABE, after the initial decrease in ^{234}Th, the $\partial^{234}\mathrm{Th}/\partial t$ term accounted for $<10\%$ of the observed ^{234}Th particle flux as determined by equation (1). Given a mean activity of total ^{234}Th of 1.8 dpm l^{-1} the ^{234}Th activity either 30 days before or after our cruise would need to differ by 0.5 dpm l^{-1} in order for the $\partial^{234}\mathrm{Th}/\partial t$ term to be of similar magnitude to the particle flux term P determined by equation (1). This temporal change is beyond that observed comparing our ^{234}Th activities with those determined within a 1 month period before or after our occupation of the 140°W line (Bacon *et al.*, 1995; Murray *et al.*, 1995). In addition, four repeat ^{234}Th casts within a two-week period in both the spring and fall during an occupation of 0°N, 140°W have led Bacon *et al.* (1995) to conclude that steady state can be assumed for ^{234}Th. For the EqPac region as a whole, the largest variations in production and export are tied to El Niño effects. The measured variations in ^{234}Th activity in 1992, between the spring and fall (El

Niño and onset of non-El Niño conditions, respectively), are not large enough to necessitate inclusion of non-steady state terms in the ^{234}Th activity balance.

Regional 3-D ^{234}Th flux model

A second model of vertical ^{234}Th flux was developed that includes physical transport. The model is based upon the ^{234}Th activity balance shown by equation (2) and the assumption of steady state (see above). This analysis requires not only ^{234}Th/^{238}U disequilibria data, but also the vertical and horizontal gradients of ^{234}Th and an estimate of appropriate vertical and horizontal velocities. The first step is to use the ^{234}Th data in Table 1 to calculate the ^{234}Th activity on a grid with a resolution of 1 degree latitude by 5 degrees longitude between 12°N to 10°S and 90°W to 175°W (the same Kriging technique is employed—Figs 1 to 6). Next, assuming the activity gradients are linear, $\partial A_{Th}/\partial x$ and $\partial A_{Th}/\partial y$ are calculated. The vertical ^{234}Th gradient, $\partial A_{Th}/\partial z$, is estimated from the ^{234}Th activity of the 0–100 m layer and the activity at the base of this layer, 100 m $[(A_{Th}^{100} - A_{Th}^{0-100})/50]$. Vertical gradients calculated in this manner are similar to those determined from discrete ^{234}Th profiles as measured by Murray *et al.* (1995) and Bacon *et al.* (1995).

Horizontal and vertical velocities are from an ocean general circulation model configured for the tropical Pacific Ocean. This model is not discussed in detail here, since it is the same physical model used by Chai *et al.* (1995) in their studies of nitrate cycling. Velocities are also averaged over the 1 × 5 degree model grid, for the spring (March–April) and fall (September–October–November) periods in 1992. Zonal and meridional velocities are averaged over 0–100 m, and the vertical velocity at 100 m is used in the calculations.

In 1992, the ocean circulation in the equatorial Pacific underwent a series of changes (McPhaden, 1993; Chai *et al.*, 1995). For example, in February the Equatorial Undercurrent was reduced to about half its normal strength, and did not return to normal until October. Such changes are not as pronounced in the depth-averaged horizonal velocities. The vertical velocity at 100 m increases from spring to fall by 1 to 2 m day^{-1} at 140°W on the equator, due to strengthening of the westward surface winds (Fig. 9). At all times, the equatorial upwelling velocities are significantly higher along 140°W relative to other transects (Fig. 9). Given ^{234}Th's 24 day half-life, its activity distribution at any one time reflects the ^{234}Th sources and sinks integrated over a period of several months, or 2–3 half-lives. Therefore, despite observation and modeling results that suggest the vertical velocity near the equator varies significantly on time scales of days to weeks (Weisberg, 1993; Harrison, 1995), it is most appropriate to use the 2–3 month time averaged vertical velocities for the ^{234}Th flux modeling.

Using equation (2), our gridded data, and the site specific estimates of u, v, and w, the particulate export flux of ^{234}Th can be calculated for the entire region. Since upwelling provides a source of ^{234}Th, it must be balanced by additional vertical export or horizontal losses. A positive horizontal velocity and an increasing ^{234}Th activity gradient towards the east result in a net loss of ^{234}Th. Similarly, positive velocities along increasing ^{234}Th activity gradients in the northward direction result in a net loss of ^{234}Th.

The relative importance of each term in equation (2) depends upon the measured ^{234}Th/^{238}U disequilibria, the magnitude and sign of the local velocity field, and ^{234}Th activity gradients. In general, the magnitude of the vertical ^{234}Th flux is dominated by the ^{234}Th/^{238}U terms except near the equator. This is coincident with the maximum upwelling

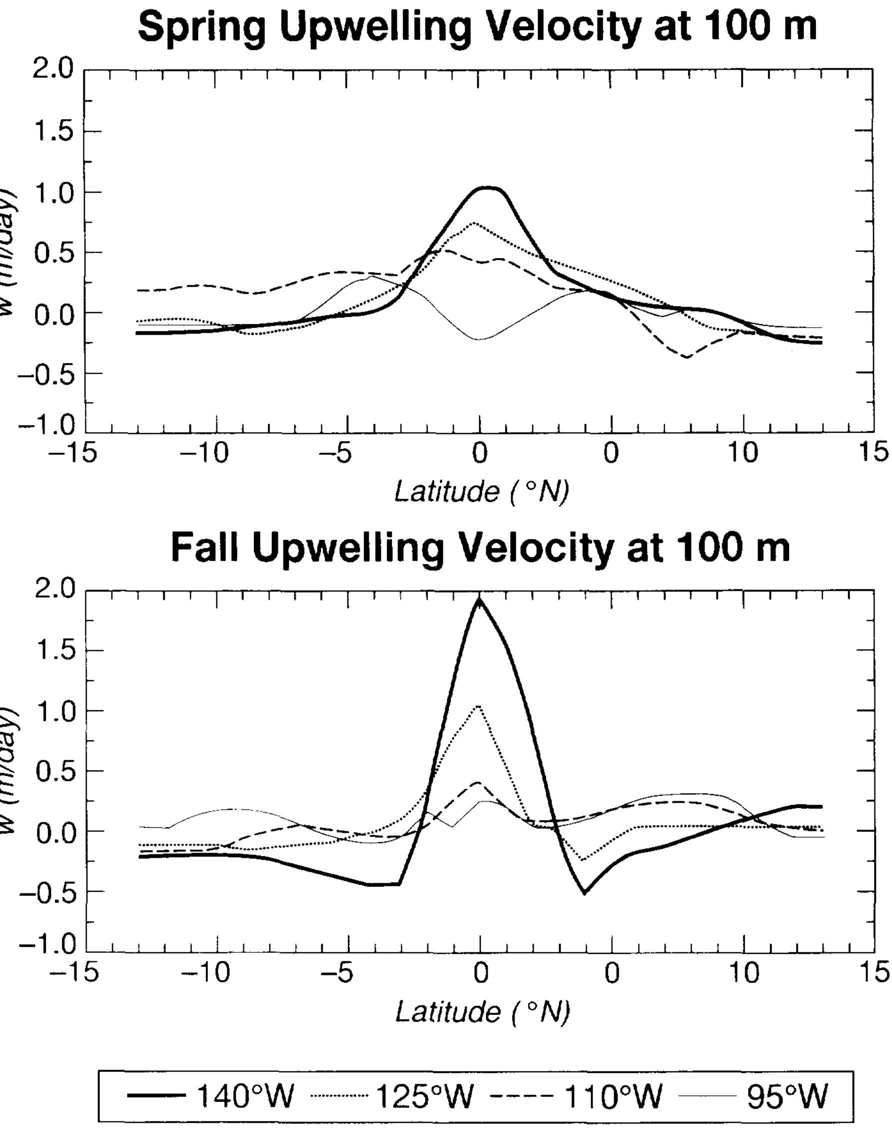

Fig. 9. Upwelling velocities at 100 m as a function of latitude for spring (upper panel) and fall (lower panel). These velocities are derived from the model used by Chai and Barber (1995), and represent the average upwelling rate in units of m day^{-1} determined at 100 m over a 2–3 month period for the spring and fall of 1992.

rates along 140°W (Fig. 10). The model predicts an increased ^{234}Th flux over the equatorial upwelling region by as much as 50% near 140°W and is slightly reduced in regions of downwelling. Zonal and meridional flux terms tend to be insignificant in the overall ^{234}Th balance, although small negative fluxes related to horizontal transport of ^{234}Th can be seen near the upwelling maximum (Fig. 10).

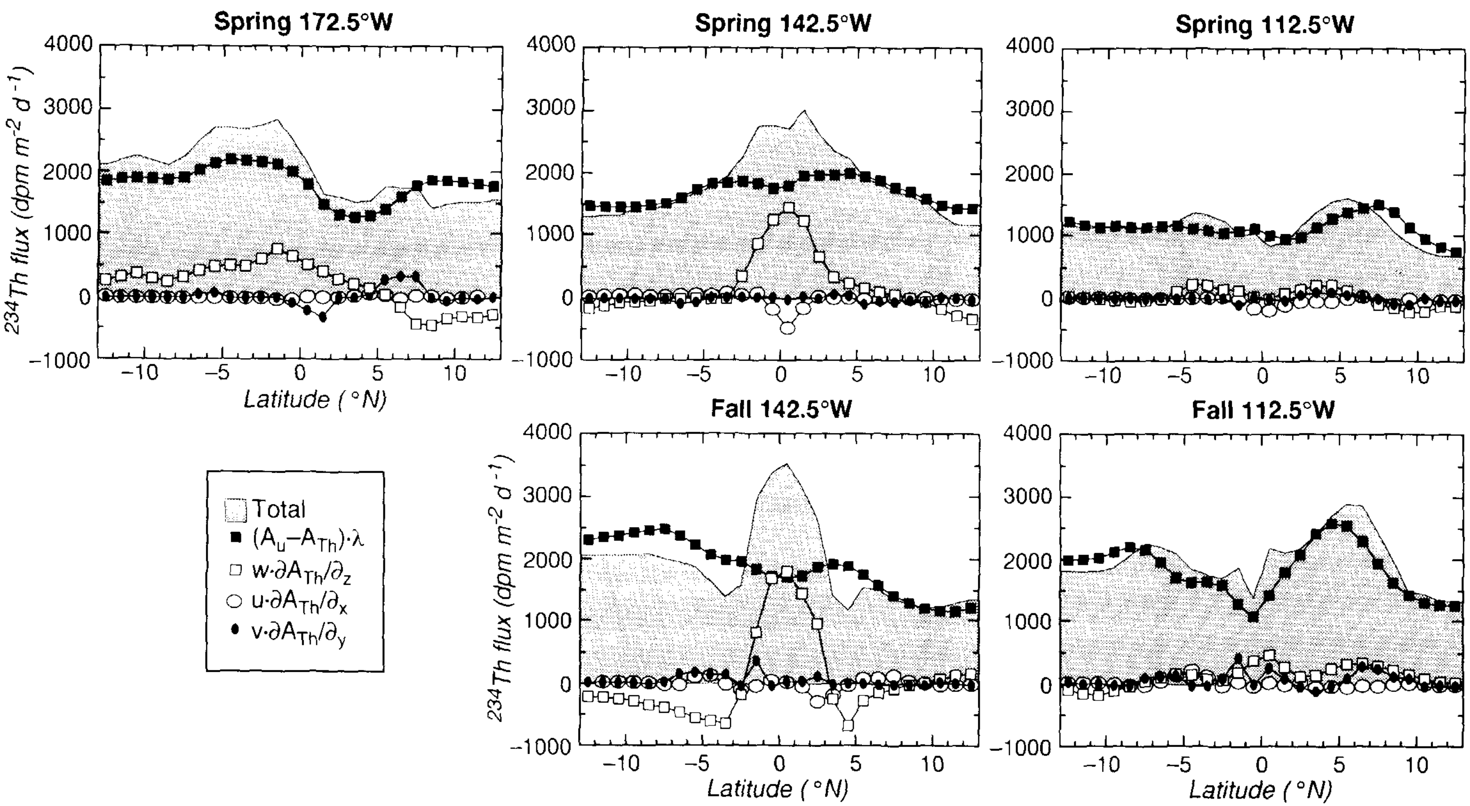

Fig. 10. Comparison of the individual ^{234}Th flux terms calculated from the 3-D regional model along three transects in the spring and two in the fall. In each panel, the total flux, shown by the shaded region, can be compared to the individual flux terms described by equation (2). A non-advective model (flux $= (A_U - A_{Th})\lambda$) would predict lower fluxes near the equator in the vicinity of 140°W (filled squares). Advective ^{234}Th fluxes are calculated for both the upwelling term (open squares), and the horizontal terms in equation (2) (open and filled circles for u and v, respectively). Fluxes are plotted in units of dpm m^{-2} day^{-1} for ^{234}Th.

Using this model, we see a tongue of high ^{234}Th flux (>2000–2500 dpm m^{-2} day^{-1}) in the spring, centered around 2°S 170°W, running just north of the equator as far east as 125°W (Fig. 8). At the same time along 140°W, we find the highest fluxes between 2°N and 2°S (>2500 dpm m^{-2} day^{-1}), and then a rapid drop to <1500 dpm m^{-2} day^{-1} at latitudes 7–8°N or S. In the fall, a similar trend is seen, though the pattern is somewhat more complicated. Higher upwelling velocities along 140°W result in some of the highest predicted ^{234}Th export fluxes (>3000 dpm m^{-2} day^{-1}). We believe that the high equatorial fluxes in this region are a real feature despite poor ^{234}Th coverage along this transect, since our extrapolated ^{234}Th activities are similar to the results found along 140°W by Murray *et al.* (1995) and Bacon *et al.* (1995). With the inclusion of upwelling, the equatorial export fluxes are 25–35% higher relative to the non-advective approach along the eastern transects (compare Figs 7 and 10). The low ^{234}Th activities centered around 5°N between 125–110°W result in locally high particle fluxes in our 3-D model, and the ^{234}Th fluxes predicted at latitudes >8°N and 8°S are not significantly different between the non-advective or advective approaches.

Including advection in the flux calculations therefore results in the prediction of enhanced particulate fluxes over equatorial upwelling regions. This pattern is consistent with the enhanced sedimentary inventory of ^{234}Th and higher deep sediment trap fluxes found below the equator along 140°W in 1992 (Pope *et al.*, 1995; Honjo *et al.*, 1995). Also, long term records of sedimentary carbonate and organic C suggest higher equatorial burial fluxes (Isern *et al.*, 1990; Martin *et al.*, 1991). Such evidence supports, at least qualitatively, the inclusion of upwelling in any ^{234}Th based model of upper ocean export in this region.

Particulate organic C/^{234}Th ratios

While the temporal and spatial distribution of ^{234}Th is by itself of interest, the derivation of particulate organic C and N export from the particulate ^{234}Th flux is the ultimate goal of this work. Eppley (1989) proposed that by using the residence time of ^{234}Th and the measured POC inventory, one could calculate the rates of new production (i.e. POC flux). This assumes that ^{234}Th and POC have similar residence times, which, as pointed out by Murray *et al.* (1989), is not generally the case. In this study, organic C flux is calculated using regional particulate ^{234}Th flux model and the empirical relationship between ^{234}Th and organic C on particles found at each station. This approach does not assume a similar behavior for particulate organic C and ^{234}Th; rather, it only assumes that the same particles responsible for the removal of ^{234}Th are also removing organic C (and associated nutrients). Confidence in this approach was first obtained during the NABE (Buesseler *et al.*, 1992a), where at least in the upper 35–75 m, the predicted organic C and N flux was similar to that determined by CO_2 drawdown and budgets of upper ocean nutrients and oxygen (Goyet and Brewer, 1993; Bender *et al.*, 1992). The advantage of this study over the NABE is that the ratios of organic C and N to ^{234}Th were determined on the exact same filters for two particle size classes, not by comparison of *in situ* pump, bottle POC and trap particulate ratios.

Since we don't know *a priori* if particulate export is driven by large rapidly sinking particles or by slowly settling material, this ratio is determined on both the 53 μm Nitex screen (LPOC/^{234}Th) and the 0.7 μm GFF filter (POC/^{234}Th). POC/^{234}Th ratios range from <2 to >4 μmol dpm^{-1} in the spring (Fig. 11), with a trend towards higher values in the NE. The pattern changes in the fall. Then, the higher values are generally in the east, with a maximum of 95°W at southern latitudes. LPOC/^{234}Th ratios range from <0.5 to >2.5 μmol dpm^{-1} in the spring. Again higher values are seen in the NE corner of the study region (Fig. 12). The fall LPOC/^{234}Th ratios span a similar range. There is a maximum, similar to the GFF filters, at 95°W at southern latitudes (Fig. 12).

These results point to two general findings: (i) the organic C to ^{234}Th ratio is higher on small relative to large particles, and (ii) the patterns of both size classes show clear regional similarities. This finding of regional similarities in the particle ratios may seem unexpected, given the widely differing patterns of organic C and ^{234}Th on the GFF filters (compare Figs 3 and 5) and the similar concentration patterns on the Nitex screen (Figs 4 and 6). Therefore it is worth considering what might drive this ratio in natural systems before we apply these ratios to our ^{234}Th flux model.

The concentration of sorbed ^{234}Th, like any surface reactive element, depends upon the number of surface binding sites and its affinity for these sites relative to remaining as a complex or free ion in solution. In general, the surface area to volume ratio decreases with increasing size. Therefore, larger particles would have a higher C/^{234}Th ratio for particles of similar composition and affinity (i.e. ^{234}Th follows surface area and C follows volume). Equal C/^{234}Th ratios between size classes are possible if larger particles are formed exclusively from the physical aggregation of smaller ones. In order for the ratio of organic C/^{234}Th to decrease with increasing size (as seen here), one would need to lose organic C preferentially during the formation of larger particles. Alternatively, the larger particles would need to have a higher affinity for ^{234}Th adsorption, as proposed by Lee *et al.* (1993).

We interpret the observed decrease in the C/^{234}Th ratio with increasing size as largely a reflection of the utilization of organic C during grazing and trophic transfer of ingested particles through the food web. In this case, "fresh" particles produced via biological production would have the highest C/^{234}Th ratios. As particles are grazed, organic C is lost. In this scenario, one would expect decreasing C/^{234}Th ratio with depth, as particles sink out of the source region and organic C is preferentially remineralized at depth. Regional or temporal changes in C/^{234}Th could occur as a function of local production and export balances. Some of the highest C/^{234}Th ratios have been found for 0.5–1 μm particles during bloom conditions, such as in the North Atlantic (14–23 μmol dpm^{-1}—Buesseler *et al.*, 1992a), or Bedford basin (>40 μmol dpm^{-1}—S. Niven, unpublished data). In the NABE, a decrease in C/^{234}Th with depth was also found (>20 to <10 between the surface and 300 m), and the C/^{234}Th ratio was 2–4 × lower in traps (which collect presumably large, sinking aggregates) relative to >0.5–1 μm particles at the same depth (Buesseler *et al.*, 1992a). These data are consistent with our hypothesis of a dominant role being played by the biota in determining the C/^{234}Th ratio, both in the production of fresh particles with high organic C, and in the grazing cycles which preferentially utilize organic C over ^{234}Th. This preferential utilization of organic C over ^{234}Th is supported by the longer overall residence times of POC vs particulate ^{234}Th in surface waters (Murray *et al.*, 1989).

During EqPac, a slight increase in C/^{234}Th is seen between the spring and fall, with the highest ratios found at 5°S 95°W (Figs 11 and 12). This ratio peak is associated with a low temperature (Fig. 1) and high nutrient region. Bacon *et al.* (1995) see a decrease in C/^{234}Th with depth in vertical profiles along 140°W, which is similar to NABE. A comparison of samples collected at 100 m with the value for the 0–100 m layer, reveals a decrease in C/^{234}Th by 40–50%. The C/^{234}Th ratio on the Nitex screen is 48% of that on GFF filters (using all ratio data with uncertainties <25% for GFF and <50% for Nitex screens). Since a Redfield organic C/N ratio was observed in the upper 100 m on both particles size classes (6.1 ± 0.6 for GFF, and 6.4 ± 0.6 for Nitex), the mean C/N ratio of 6.3 mol/mol can be used to convert the particulate flux of organic C to N.

Estimates of particulate organic carbon export

The basis for the quantification of particulate organic C export from ^{234}Th is an empirical one. It assumes that the same particles which are removing ^{234}Th are also carrying organic C and associated nutrients to depth. Seasonal and site specific estimates of both ^{234}Th flux and the local particulate organic C/^{234}Th ratios are therefore required. We base our best estimate of POC flux upon the regional 3-D model and the organic C/^{234}Th ratio data from the large particle pool. Overall, it is predicted that POC fluxes are on the order of 2–4 mmol m^{-2} day^{-1} in the spring. A band of elevated POC export is seen stretching from the equatorial region between 170 and 140°W, to somewhat north of the equator east of 140°W in the direction of the Guatemala basin (Fig. 13). In the fall, the fluxes are 2–4 mmol m^{-2} day^{-1}, except along 95°W, where enhanced export >7 mmol m^{-2} day^{-1} is found. This is associated with the region of highest C/^{234}Th ratios (and elevated nutrients). The pattern in the fall is also somewhat more complex. There is enhanced export associated with elevated ^{234}Th fluxes along 110°W, north of the equator.

Some constraints can be placed on these POC flux estimates by examining the two factors which are used to calculate this flux, namely the ^{234}Th flux and the C/^{234}Th ratio. As stated in the modeling section, the magnitude of the ^{234}Th flux is dominated by the measured ^{234}Th/^{238}U ratio at any given site and time. When upwelling is included, it is clear that at some sites along the equator, the flux is sensitive to the chosen value of w. This sensitivity can be examined by recalculating the organic C fluxes with an upwelling rate that is a factor of two higher or lower than that used by Chai *et al.* (1995). In this sensitivity analysis, u and v are ignored given their relatively small influence on the ^{234}Th models (Fig. 10). This analysis suggests that except near the equator, close to 140°W, a variation in w by a factor of two has a small effect on the estimate of the particulate organic C flux (Fig. 14). At the equator, along 140°W, a doubling of w increases organic C fluxes by up to 50%, while a reduction in w by a factor of two decreases the predicted flux by 25%. One might argue that the estimates of w are less well constrained than $\pm$ a factor of two. However, even if upwelling rates were five times larger, the predicted organic C flux would increase by less than a factor of three. Furthermore, this difference would only be significant near the equator and 140°W, and not at those sites further north or south, or more distant from this upwelling maximum.

The second constraint on the export prediction is related to how well we can measure the particulate organic C/^{234}Th ratio, which is representative of the sinking particle pool. A change in this ratio will directly affect the predicted flux by the same magnitude. In the analysis shown in Fig. 13, the LPOC/^{234}Th ratio is used. As stated previously, if the POC/^{234}Th ratio is used, the fluxes would be a factor of two higher, and if the same ratios from 100 m are used (rather than the average of the 0–100 m layer), the flux would decrease by a factor of two. With these data, we can therefore place bounds on the export flux. The ratios of C/^{234}Th in the different pools vary systematically, so the regional pattern of organic C export would not differ dramatically if a different C/^{234}Th ratio was used, only the overall magnitude would change.

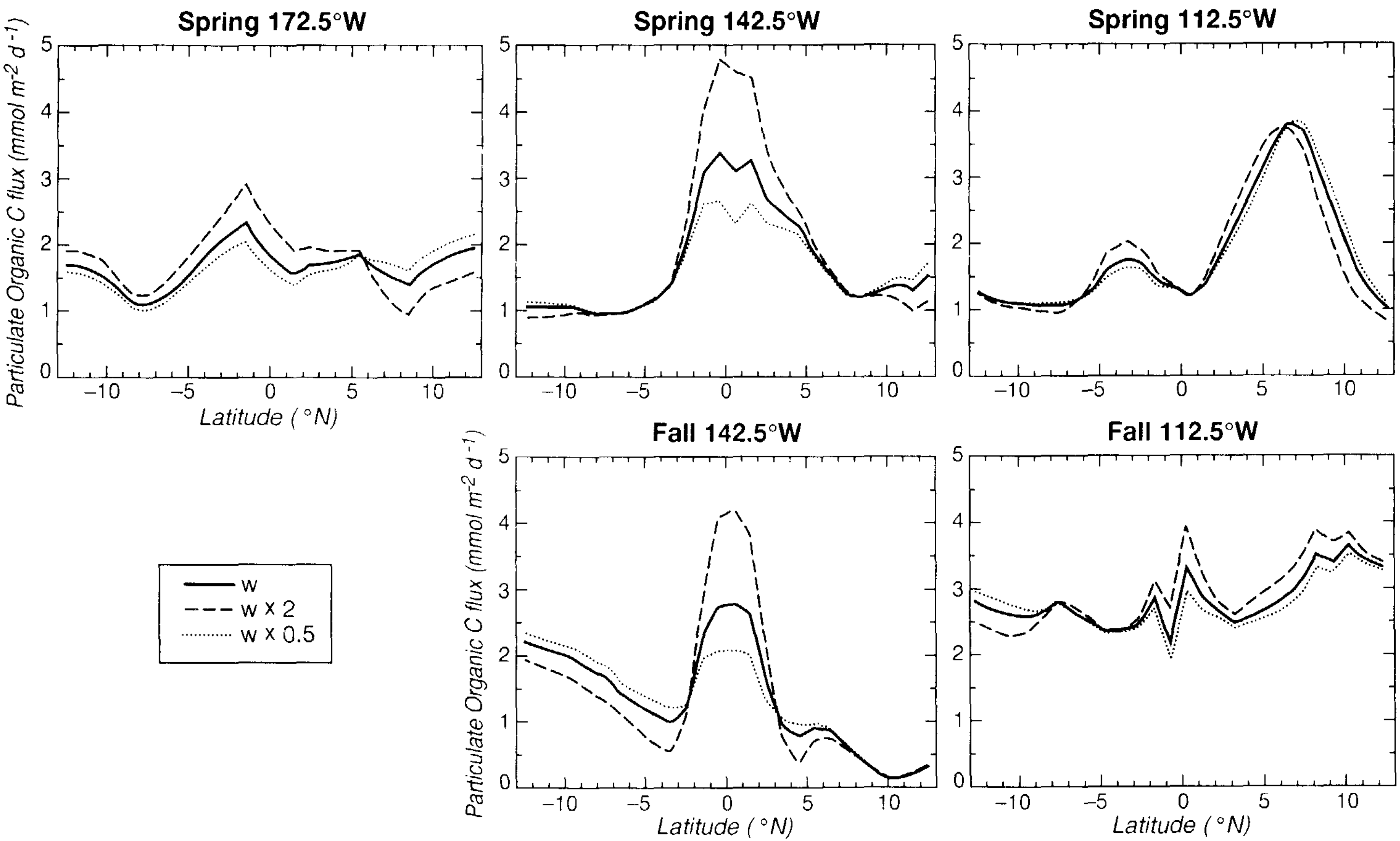

Fig. 14. Sensitivity of the calculated organic C flux to variations in upwelling rate along three transects in the spring (172.5°W, 142.5°W, and 112.5°W) and two in the fall (142.5°W and 112.5°W). In each panel, the magnitude of the organic C flux determined by the 3-D regional model is shown by the heavy solid line. The organic C flux was recalculated for an upwelling velocity 2× higher (dashed line) and 2× lower (dotted line).

Relationship to other studies. A wide variety of scientists are working to constrain the budgets of inorganic and organic carbon and associated nutrients in the EqPac program. Many of these results are being published for the first time in this volume and an evaluation of the entire carbon budget for this experiment will then be possible. However, a preliminary assessment of the carbon balance can already be made.

Focusing on the spring data at 140°W at the equator, Feely *et al.* (1995) estimate from DIC data that on the order of 14 ± 6 mmol m^{-2} day^{-1} of total C are lost from the upper 100 m by all processes. These loss processes include gas exchange, DOC/POC advection, and vertical settling of POC. Gas exchange is thought to account for 2–3 mmol C m^{-2} day^{-1} (Feely *et al.*, 1995) and is a relatively small term in the C balance. Peltzer and Hayward (1995) used DOC data to suggest that 4–8 mmol C m^{-2} day^{-1} is lost due to advection of total organic C (DOC and POC). Our estimate of the sinking flux of POC at 100 m is 3–4 mmol C m^{-2} day^{-1} from ^{234}Th for this site and time. Bacon *et al.* (1995) estimate the POC flux at 120 m to be 2 mmol C m^{-2} day^{-1} using ^{234}Th data collected one month prior to ours. While the uncertainty in any of these estimates is high, due in part to the uncertainty in the chosen upwelling velocities and the 1-D approach taken by most of these studies, there is a general agreement that the export flux of sinking particles is not the major loss term for carbon during the EqPac study.

The net source of organic C in surface waters is primary production. Carbon-14 and ^{13}C estimates of total primary production are on the order of 50–80 mmol m^{-2} day^{-1} at the equator along 140°W, dropping off by roughly 50% towards latitudes >8°N and 8°S (Barber *et al.*, 1995; Chavez *et al.*, personal communication). Along 140°W, there is a range of new production estimates using ^{15}N techniques, but all of these values are significantly larger (10–20 mmol m^{-2} day^{-1}—McCarthy, 1995) than the ^{234}Th derived particle export fluxes. The general conclusion is that a significant fraction of total production leaves the equator as a horizonal advective DOM flux, rather than a vertical POC flux. Since we do not see any specific site of increased particle export off of the equator in our ^{234}Th data, we must speculate that surface water production that is fueled by upwelling at the equator is ultimately removed far afield, possibly along the eastern margins of this basin.

The final point to be made is that all of the production and export estimates indicate elevated fluxes over the equator, at least along 140°W. This pattern also is reflected in the deep water traps and sedimentary signals. For example, our spring time particulate organic C fluxes at 100 m peak along 140°W at 3–4 mmol m^{-2} day^{-1}, and decrease to 1 mmol m^{-2} day^{-1} by 5–7°N or S. The >2000 m sediment trap data from Honjo *et al.* (1995) for the same season also show an equatorial peak in particle flux; however, by 2200 m, the organic C flux is reduced to approximately 0.5 mmol m^{-2} day^{-1} at the equator, to <0.1–0.2 mmol m^{-2} day^{-1} further north and south. In the sediments, EqPac investigators have found peak ^{234}Th inventories underlying the equator (Pope *et al.*, 1995), and benthic respiration rates which are enhanced between 2°N and 2°S (Berelson, personal communication). When making this comparison it is worth noting that all of these flux estimates average over time scales of 1–3 months. The magnitude of, and latitudinal patterns in the long term benthic accumulation rates may differ depending upon seasonal and inter-annual variations in production and local diagenetic effects.

CONCLUSIONS

We have been able to estimate the flux of particulate organic C and N from the upper 100 m during the spring and fall of 1992 for a large region of the equatorial Pacific. To make this estimate, ^{234}Th data are used to constrain the ^{234}Th particle flux and the empirical ratio of organic C and N to ^{234}Th on both large and small particles is used to estimate particulate organic C and N export. The ^{234}Th flux estimates are obtained from a regional 3-D model that includes site specific estimates of upwelling and horizontal advection which are used with the measured ^{234}Th activity gradients to calculate the ^{234}Th flux. We find that the ^{234}Th flux does not change dramatically between the spring and fall, and that particle fluxes are higher in general over the upwelling regions. Export fluxes of particulate organic C range between 2 and 7 mmol C m^{-2} day^{-1}. Along 140°W, an equatorial peak of 3–4 mmol m^{-2} day^{-1} is found in the spring that is 2–3 × higher than the flux at latitudes >8 degrees north or south. The highest export fluxes are centered around 5°S 95°W in the fall, where significantly lower temperatures and higher nutrients are found.

The magnitude of the particulate organic C flux is determined by three factors: the measured ^{234}Th and POC/PON concentrations; the specific estimates of upwelling included in the ^{234}Th model; and whether we use the small or large particle organic C/^{234}Th ratio to convert from ^{234}Th export to C flux. In our final analysis, we assume that the POC/^{234}Th ratio of the larger and (presumably) rapidly settling particles is the most appropriate for estimating organic C export. The POC/^{234}Th ratio is constrained better than a factor of two, which is the difference between the smaller 0.7 μm particles which have higher ratios, and the filters collected at the 100 m layer which have 50% lower ratios than the 0–100 m average. If upwelling rates are increased by a factor of two, the POC flux would increase over the equator by 50% along 140°W; however, the sensitivity of the predicted fluxes to the chosen value of w is much smaller elsewhere in this region.

Our conclusion is that during the EqPac study, particle export from the upper 100 m is small. These data suggest that only a small percentage of the carbon fixed during production is being exported locally on sinking particles, and much of the export may be occurring as advective transport of DOM. We feel that the ^{234}Th approach is a relatively simple and robust procedure for determining quantitative particle export fluxes for organic C and associated nutrients over large spatial scales. However, future studies aimed at further understanding the relationship between organic C and ^{234}Th on sinking particles are warranted.

Acknowledgements—The authors are pleased to acknowledge the assistance of J. F. Todd, S. B. Moran, and S. Casso for their participation in the EqPac sampling cruises and E. Peltzer for DOC analyses. Efforts by the chief scientists, officers and crew of the R.V. *Malcolm Baldridge* and R.V. *Discoverer* contributed greatly to the success of this program. The authors would also like to thank S. Clifford and J. Ducette at WHOI for assistance in preparing the text and graphics in this paper. The *in situ* pumping system was designed and produced by B. Hamblin and co-workers of Oceanic Industries, Inc. Discussions with M. Bacon, J. K. Cochran and J. Murray regarding relevant issues of thorium intercalibration and modeling are also highly appreciated. K.O.B. was supported by a grant from the NOAA Climate and Global Change Program. This is contribution No. 8919 from the Woods Hole Oceanographic Institution, and JGOFS contribution No. 161.

REFERENCES

Bacastow R. and E. Maier-Reimer (1991) Dissolved organic carbon in modeling oceanic new production. *Global Biogeochemical Cycles*, **5**, 71–85.

Bacon M. P., J. K. Cochran, D. Hirschberg, T. R. Hammar and A. P. Fleer (1995) Export flux of carbon at the equator during the EqPac time-series cruises estimated from ^{234}Th measurements. *Deep-Sea Research*, (submitted).

Barber R. T., M. P. Sanderson, S. T. Lindley, F. Chai, J. Newton and F. P. Chavez (1995) Primary production in the equatorial Pacific along 140°W. *Deep-Sea Research II*, (submitted).

Bender M., H. Ducklow, J. Kiddon, J. Marra and J. Martin (1992) The carbon balance during the 1989 spring bloom in the north Atlantic Ocean, 47°N, 20°W. *Deep-Sea Research*, **39**, 1707–1725.

Bhat S. G., S. K. Krishnaswamy, D. Lal, D. Rama and W. S. Moore (1969) ^{234}Th/^{238}U ratios in the ocean. *Earth and Planetary Science Letters*, **5**, 483–491.

Bishop J. K. B., M. Q. Fleisher and A. Ingalls (1995) Distributions and chemistry of biogenic particulate matter in the central equatorial Pacific: Response to El Niño forcing. *Deep-Sea Research*, (submitted).

Bishop J. K. B. and J. M. Edmond (1976) A new large volume filtration system for the sampling of oceanic particulate matter. *Journal of Marine Research*, **34**, 181–198.

Buesseler K. O., M. P. Bacon, J. K. Cochran and H. D. Livingston (1992a) Carbon and nitrogen export during the JGOFS North Atlantic Bloom Experiment estimated from ^{234}Th:^{238}U disequilibria. *Deep-Sea Research I*, **39**, 1115–1137.

Buesseler K. O., J. K. Cochran, M. P. Bacon, H. D. Livingston, S. A. Casso, D. Hirschberg, M. C. Hartman and A. P. Fleer (1992b) Determination of thorium isotopes in seawater by non-destructive and radiochemical procedures. *Deep-Sea Research*, **39**, 1103–1114.

Buesseler K. O., A. F. Michaels, D. A. Siegel and A. H. Knap (1994) A three dimensional time-dependent approach to calibrating sediment trap fluxes. *Global Biogeochemical Cycles*, **8**, 179–193.

Chai F., S. T. Lindley and R. T. Barber (1995) Origin and maintenance of high nitrate condition in the equatorial Pacific. *Deep-Sea Research II*, (submitted).

Chavez F. P. and R. T. Barber (1987) An estimate of new production in the equatorial Pacific. *Deep-Sea Research I*, **34**, 1129–1243.

Chen J. H., R. L. Edwards and G. J. Wasserburg (1986) ^{238}U, ^{234}U and ^{232}Th in seawater. *Earth and Planetary Science Letters*, **80**, 241–251.

Coale K. H. and K. W. Bruland (1985) ^{234}Th:^{238}U disequilibria within the California Current. *Limnology and Oceanography*, **30**, 22–33.

Coale K. H. and K. W. Bruland (1987) Oceanic stratified euphotic zone as elucidated by ^{234}Th:^{238}U disequilibria. *Limnology and Oceanography*, **32**, 189–200.

Eppley R. W. (1989) New production: History, methods, problems. In *Productivity of the ocean: Present and past*. W. H. Berger, V. S. Smetacek and G. Wefer, editors, John Wiley, New York, U.S.A., pp. 85–97.

Feely R. A., R. Wanninkhof, C. E. Cosca, P. P. Murphy, M. F. Lamb and M. D. Steckley (1995) CO_2 distributions in the equatorial Pacific during the 1991–1992 ENSO event. *Deep Sea Research II*, **42**, 365–386.

Goyet C. and P. G. Brewer (1993) (unpublished data). Temporal variations of the properties of the carbonate system in the North Atlantic Ocean at 47°N 20°W: II. The Process Study.

Harrison D. E. (1995) Vertical velocity in the central tropical Pacific—a circulation model perspective for JGOFS. *Deep-Sea Research II*, (submitted).

Hartman M. C. and K. O. Buesseler (1994) Adsorbers for in-situ Collection and At-Sea Gamma Analyses of Dissolved Thorium-234 in Seawater: WHOI Technical Report 94-15, Woods Hole Oceanographic Institution, Woods Hole, MA, U.S.A., 19 pp.

Honjo S., J. Dymond, R. Collier and S. J. Manganini (1995) Export production of particles to the interior of the equatorial Pacific Ocean during the 1992 EqPac experiment. *Deep-Sea Research II*, **42**, 831–860.

Isern A., M. Leinen, W. Martin and M. Bender (1990) Glacial to interglacial changes in the accumulation of organic carbon and carbonate in the central equatorial Pacific Ocean. *Eos, Transactions of the American Geophysical Union*.

Kaufman A., Y.-H. Li and K. K. Turekian (1981) The removal rates of ^{234}Th and ^{228}Th from waters of the New York Bight. *Earth and Planetary Science Letters*, **54**, 385–392.

Ledwell J. R., A. J. Watson, K. W. Doherty and W. M. Berelson (1991) Integrating Samplers for the Deep Sea. *Journal of Geophysical Research*, **96**, 8727–8732.

Lee T., E. Barg, D. Lal and F. Azam (1993) Bacterial scavenging of ^{234}Th in surface ocean waters. *Marine Ecology Progress Series*, **96**, 109–116.

Legendre L. and M. Gosselin (1989) New production and export of organic matter to the deep ocean: Consequences of some recent discoveries. *Limnology and Oceanography*, **34**, 1374–1380.

Livingston H. D. and J. K. Cochran (1987) Determination of transuranic and thorium isotopes in ocean water: in solution and in filterable particles. *Journal of Radioanalytical and Nuclear Chemistry*, **115**, 299–308.

Martin W., M. Bender, M. Leinen and J. Orchardo (1991) Benthic fluxes of NO_3^-, SiO_2, and O_2 across the equatorial high productivity zone at 135°W. *Deep-Sea Research I.*

McCarthy J. J. (1995) Equatorial new production along 140°W during and following the 1992 El Niño. *Deep-Sea Research II*, (in prep).

McPhaden M. J. (1993) TOGA–TAO and the 1991–92 ENSO event. *Oceanography*, **6**, 36–44.

Minagawa M. and S. Tsunogai (1980) Removal of ^{234}Th from a coastal sea: Funka Bay, Japan. *Earth and Planetary Science Letters*, **47**, 51–64.

Murray J. W., J. N. Downs, S. Strom, C.-L. Wei and H. W. Jannasch (1989) Nutrient assimilation, export production and ^{234}Th scavenging in the eastern equatorial Pacific. *Deep-Sea Research I*, **36**, 1471–1489.

Murray J. W., M. W. Leinen, R. A. Feely, J. R. Toggweiler and R. Wanninkhof (1992) EqPac: A process study in the central equatorial Pacific. *Oceanography*, **5**, 134–142.

Murray J. W., R. T. Barber, M. R. Roman, M. P. Bacon and R. A. Feely (1994) Physical and biological controls on carbon cycling in the Equatorial Pacific. *Science*, **266**, 58–65.

Murray J. W., J. Young, J. Newton, J. Dunne, T. Chapin and B. Paul (1995) Export flux of particulate organic carbon from the central equatorial Pacific determined using a combined drifting trap-^{234}Th approach. *Deep-Sea Research II*, (in prep).

Peltzer E. T. and N. A. Hayward (1995) Spatial distribution and temporal variability of total organic carbon along 140°W in the Equatorial Pacific Ocean in 1992. *Deep-Sea Research II*, (submitted).

Pope R., D. DeMaster, C. Smith, S. Doan, D. Hoover and S. Garner (1995) Biological mixing and particle flux along the JGOFS 140°W transect: evidence from the Th-234 distributions in the seabed. *Deep-Sea Research II*, (in prep).

Santschi P. H., Y.-H. Li and J. Bell (1979) Natural radionuclides in the water of Narragansett Bay. *Earth and Planetary Science Letters*, **45**, 201–213.

Toggweiler J. R. (1989) Is the Downward Dissolved Organic Matter (DOM) Flux Important in Carbon Transport? In *Productivity of the ocean: Present and past*, W. H. Berger, V. S. Smetacek and G. Wefer, editors, John Wiley, New York, U.S.A., pp. 65–83.

Weisberg (1993) (unpublished data) Proceedings Report: EqPac Data and Science Workshop No. 1.